

See discussions, stats, and author profiles for this publication at: <https://www.researchgate.net/publication/7304408>

# Composite phospholipid–calcium carbonate microparticles: Influence of anionic phospholipids on the crystallization of calcium carbonate

ARTICLE *in* THE JOURNAL OF PHYSICAL CHEMISTRY B · MARCH 2006

Impact Factor: 3.3 · DOI: 10.1021/jp056865m · Source: PubMed

---

CITATIONS

12

---

READS

33

## 4 AUTHORS, INCLUDING:



Zonghuan Lu

Rensselaer Polytechnic Institute

25 PUBLICATIONS 479 CITATIONS

SEE PROFILE



Melgardt M De Villiers

University of Wisconsin–Madison

130 PUBLICATIONS 2,089 CITATIONS

SEE PROFILE



Yuri M Lvov

Louisiana Tech University

292 PUBLICATIONS 13,971 CITATIONS

SEE PROFILE

# Synthesis of Size-Controlled Monodisperse Manganese Carbonate Microparticles as Templates for Uniform Polyelectrolyte Microcapsule Formation

Huiguang Zhu,\* Erich W. Stein, Zonghuan Lu, Yuri M. Lvov, and Michael J. McShane

*Institute for Micromanufacturing and Biomedical Engineering Program, Louisiana Tech University,  
911 Hergot Avenue, Ruston, Louisiana 71272*

*Received October 10, 2004. Revised Manuscript Received February 23, 2005*

Inorganic colloids are usually prepared via precipitation reactions, which involve two sequential steps: nucleation and growth of the nuclei. On the basis of this theory, preformed manganese carbonate nanoseeds were prepared by mixing diluted ammonium hydrogen carbonate with manganese sulfate solution to serve as nuclei for production of monodisperse manganese carbonate microparticles. It was found that the average particle diameter can be finely tuned from 1 to 10  $\mu\text{m}$  by adding a different volume of nanoseed solution. It was further verified that the manganese carbonate microparticles can be used as templates for efficient formation of uniform, smooth multilayer polyelectrolyte microcapsules, which are promising systems for biomedical and other applications, such as biosensors, bioreactors, and drug-delivery devices.

## 1. Introduction

Polyelectrolyte microcapsules, produced by stepwise adsorption of oppositely charged polymers onto the surface of colloidal particles followed by core dissolution, are currently being studied intensively.<sup>1</sup> This base technology has recently inspired considerable attention in the fields of drug delivery, biosensors, microreactors, and bioseparations.<sup>2</sup> Using this approach, a variety of materials, including charged and uncharged species, have been successfully assembled into nanoscale multilayered structures. Furthermore, removal of the dissolved cores provides more space for material encapsulation, and the polyelectrolyte coating may function as a protective shell for encapsulated species. Different colloidal templates have been introduced for the fabrication of such microcapsules, ranging from polymers<sup>3</sup> and metal particles<sup>4</sup> to crystals of proteins,<sup>2b</sup> low molecular weight

compounds,<sup>5</sup> and biological cells.<sup>6</sup> Polystyrene (PS), silica, gold, and melamine formaldehyde (MF) spheres have been most commonly used for fundamental studies of multilayer capsules formation, because they can be commercially obtained in relatively large quantities with rather narrow size distribution and reasonable cost from many sources.

However, problems remain with the dissolution of materials to produce clean capsules. Most commercially available templates such as MF and PS require harsh conditions such as strong acids or organic solvents to be dissolved, and in some cases template materials cannot be completely removed from the capsules because of interaction with capsule walls.<sup>7</sup> Additionally, the dissolution is unpredictable because of increased cross-linking of polymer materials with time, as occurs with MF. It is believed that the MF oligomers, a product of acidic hydrolysis, lead to an increased osmotic pressure during dissolution and therefore affect the integrity of the capsule wall. The amount of MF bound to the capsule wall is hard to control and the formation of MF/polyion complex is undesirable since it makes capsules unsuitable for biomedical applications. In PS template with bioactive coatings such as proteins, the function might be affected by the organic solvent applied to dissolve the cores. Thus, improved templates are essential for efficient production of high-quality capsules.

Metal carbonates, especially calcium carbonate, have been intensively investigated in recent years because of their

\* Corresponding author. Phone: (318) 257-5127; fax: (318) 257-5104; e-mail: hzhu@latech.edu.

- (1) (a) Decher, G. *Science* **1997**, *277*, 1232. (b) Sukhorukov, G. B.; Donath, E.; Lichtenfeld, H.; Knippel, E.; Knippel, M.; Möhwald, H. *J. Colloid Surf., A* **1998**, *137*, 253. (c) Sukhorukov, G. B.; Donath, E.; Davis, S.; Lichtenfeld, H.; Caruso, F.; Popov, V. I.; Möhwald, H. *Polym. Adv. Technol.* **1998**, *9*, 759.
- (2) McShane, M. J.; Lvov, Y. M. Layer-by-Layer Electrostatic Self-Assembly. In *Encyclopedia of Nanoscience and Nanotechnology*, volume 5; Marcel Dekker: New York, 2004. (b) Moya, S.; Dahne, L.; Voigt, A.; Leporatti, S.; Donath, E.; Möhwald, H. *Colloids Surf., A* **2001**, *27*, 183. (c) Caruso, F.; Trau, D.; Möhwald, H.; Renneberg, R. *Langmuir* **2000**, *16*, 1485. (d) McShane, M. J.; Brown, J. Q.; Guice, K. B.; Lvov, Y. M. *J. Nanosci. Nanotechnol.* **2002**, *2*, 411. (e) Balabushevich, N. G.; Tiourina, O. P.; Volodkin, D. V.; Larionova, N. I.; Sukhorukov, G. B. *Biomacromolecules* **2003**, *4* (5), 1191. (f) Shchukin, D.; Shutava, T.; Sukhorukov, G.; Lvov, Y. M. *Chem. Mater.* **2004**, *16*, 3446.
- (3) (a) Donath, E.; Sukhorukov, G. B.; Caruso, F.; Davis, S. A.; Möhwald, H. *Angew. Chem., Int. Ed.* **1998**, *37*, 2201. (b) Caruso, F.; Caruso, R. A.; Möhwald, H. *Science* **1998**, *282*, 1111. (c) Dinesh, B. S.; Alexei, A. A.; Sukhorukov, G. B.; Möhwald, H. *Biomacromolecules* **2003**, *4*, 265.
- (4) Gittins, D. I.; Caruso, F. *Adv. Mater.* **2000**, *12*, 1947.

- (5) Caruso, F.; Yang, W.; Trau, D.; Renneberg, R. *Langmuir* **2000**, *16*, 8932.
- (6) (a) Moya, S.; Donath, E.; Sukhorukov, G. B.; Auch, M.; Baumler, H.; Lichtenfeld, H.; Möhwald, H. *Macromolecules* **2000**, *33*, 4538. (b) Caruso, F. *Chem. Eur. J.* **2000**, *6*, 413.
- (7) (a) Gao, C. Y.; Donath, E.; Möhwald, H.; Shen, J. C. *Angew. Chem., Int. Ed.* **2002**, *41*, 3789. (b) Gao, C. Y.; Liu, X. Y.; Shen, J. C.; Möhwald, H. *Chem. Commun.* **2002**, *17*, 1928. (c) Balabushevich, N. G.; Tiourina, O. P.; Volodkin, D. V.; Larionova, N. I.; Sukhorukov, G. B. *Biomacromolecules* **2003**, *4*, 1191.

abundance in nature and also their important industrial applications in paints, plastics, rubber, and paper.<sup>8</sup> These inorganic carbonate crystal materials are also advantageous for the formation of polymeric micro/nanocapsules,<sup>9</sup> as they can be synthesized from simple reactions, even those as simple as mixing two chemical solutions. More importantly, they can be dissolved under mild conditions to obtain clean capsules because the metal ions will not interact with polyelectrolyte walls and form complexes such as MF oligomers. For example, carbonate cores can be dissolved with EDTA solution<sup>8b</sup> without adding acid, which is an additional advantage of the carbonate crystals when employed for making capsules from pH-sensitive species such as enzymes and nucleic acids.<sup>10</sup> As demonstrations of the potential of these materials, Hamada<sup>11</sup> and Antipov<sup>8b</sup> recently reported the synthesis of manganese carbonate particles; however, these had a broad size distribution and a separation procedure was therefore needed to reach reasonable uniformity. Additionally, it is not possible to obtain repeatable particle sizes even under identical reaction conditions. As a result of having to dispose of large parts of the sample to achieve the desired distribution/particle size, this process is inefficient and wasteful of materials.

In this study, a novel technique for the preparation of spherical monodisperse  $\text{MnCO}_3$  microparticles of a desired size is described. Inorganic colloids are usually prepared via precipitation reactions, a process that often involves two sequential steps: nucleation and growth of the nuclei.<sup>12</sup> To control the crystal growth and obtain monodisperse colloids, nuclei are needed. On the basis of this nucleation and nuclei growth theory, preformed manganese carbonate nanoseeds were prepared to serve as nuclei for production of monodisperse manganese carbonate microparticles. The positively charged particles can be produced with tunable diameters between 1 and 10  $\mu\text{m}$  by adding different volumes of nanoseed solution and without further need for a separation procedure. Thus, a more efficient and delicate controllable technique for production of colloidal template was built, which shows high potential for commercial batch production. It was further verified that those manganese carbonate microparticles can be used as templates for efficient formation of uniform, smooth multilayer polyelectrolyte microcapsules, which are promising systems for biomedical and other applications, such as biosensors, bioreactors, and drug-delivery devices.

## 2. Experimental Section

**Materials.** Ammonium hydrogen carbonate and manganese(II) sulfate monohydrate were purchased from Fluka and Sigma, respectively. 2-Propanol (IPA) was from EMD Chemicals Inc.

Sodium poly(styrene sulfonate) (PSS, Mw  $\sim 70\,000$ ) and poly-(allylamine hydrochloride) (PAH, Mw  $\sim 70\,000$ ) were obtained from Aldrich. For confocal fluorescence microscopy, PAH was labeled with fluorescein isothiocyanate (FITC, Aldrich) in pH 8.5 sodium bicarbonate buffer and was precipitated in acetone.

**Synthesis of  $\text{MnCO}_3$  Microparticles.**  $\text{MnCO}_3$  crystals precipitate when mixing  $\text{NH}_4\text{HCO}_3$  with  $\text{MnSO}_4$  solution. To control the crystal shape and sizing, rapid stirring must be applied. In a typical reaction, a nanoseed solution was first prepared by mixing 4 mg  $\text{NH}_4\text{HCO}_3$  with 0.1 mg  $\text{MnSO}_4$  in 20 mL DI water with stirring. Then, 1 L of 6 mM  $\text{MnSO}_4$  in DI water (with 0.5% IPA) was mixed with 1 L of 0.06 M  $\text{NH}_4\text{HCO}_3$  in DI water (with 0.5% IPA), under rapid stirring ( $\sim 2000$  rpm) at 50 °C. To control the particle size, different volumes of nanoseed solution were added into  $\text{MnSO}_4$  solution prior to mixing. The mixed solution was then cooled to room temperature and neutralized by HCl. The particles were allowed to precipitate for at least 30 min, depending on the target particle size, followed by triple rinsing with DI water. The particles were then air-dried at 60 °C for 24 h and stored in microcentrifuge tubes until use. The yield of  $\text{MnCO}_3$  particles is about 65%, with 1.22 g  $\text{MnSO}_4$  used and 0.6 g  $\text{MnCO}_3$  produced.

**Fabrication of PSS/PAH Multilayers on  $\text{MnCO}_3$  Templates.** The PSS and PAH solutions used for multilayer assembly were prepared in DI water at 2 mg/mL. The  $\text{MnCO}_3$  particles were suspended in DI water via vortexation and ultrasonication for 10 min prior to layer-by-layer (LbL) assembly. The particles were coated with four bilayers of {PSS/PAH}, where each adsorption step reaction time was 20 min, followed by triple rinsing with DI water. The  $\text{MnCO}_3$  cores were dissolved by 0.1 M HCl solution, followed by 0.01 M EDTA solution to remove residual manganese ions. The microcapsules obtained were again triple rinsed with DI water.

**Instrumentation and Measurement.** Nanoseeds were measured with a microelectrophoretic particle sizer (90Plus Particle Sizer, Brookhaven Instruments Corp) prior to the fabrication of each  $\text{MnCO}_3$  particle batch. Bright-field optical and fluorescence microscopy (Nikon ECLIPSE TE2000-U) were used to image the  $\text{MnCO}_3$  particles with 60 $\times$  and 100 $\times$  oil immersion objectives. Scanning electronic microscopy (SEM, Amray 1830) was also used to image the nanoseeds,  $\text{MnCO}_3$  particles,  $\text{MnCO}_3$  particles with polyelectrolyte coating, and hollow microcapsules after core dissolution, with elemental analysis using energy-dispersive X-ray spectroscopy (EDX, EDS, iXRF systems, Inc.). The particle samples were dried on coverslips and sputter-coated with Au–Pd alloy. The acceleration potentials used to collect SEM images was 20 KV in our study. The size distribution of the microparticles was measured with a Coulter counter (Beckman Z2 Coulter particle count and size analyzer). The sample is made by putting 10  $\mu\text{L}$  of particle suspension in 10 mL of PBS solution and measured with a 100- $\mu\text{m}$  aperture. At least 2000 particles were counted to plot a reliable size distribution for each sample. The assembly of polyelectrolyte layers on colloidal templates was monitored by electrophoretic mobility measurements (ZetaPlus Zeta Potential Analyzer, Brookhaven Instrument Corp.). Confocal fluorescence micrographs were collected with a Leica TCS SP2 laser scanning system, equipped with a 63 $\times$  oil immersion objective. Microcapsule samples were dried on mica substrate overnight at room temperature for atomic force microscopy (AFM, Q-Scope, Model 250, QUESANT Instrument Corp.). The imaging was performed in the noncontact mode (or tapping mode) with an NSC16 silicon cantilever. In the tapping mode setting, a minimum damping of 50% was selected and a scan frequency of 1.5 Hz and a scan resolution of 600 lines/scan were used to collect the images.

- (8) Dalas, E.; Klepetsanis, P.; Koutsoukos, P. G. *Langmuir* **1999**, *15*, 8322.
- (9) (a) Silvano, D.; Krol, S.; Diaspro, A.; Cavalleri, O.; Gliozzi, A. *Microsc. Res. Tech.* **2002**, *59*, 536. (b) Antipov, A. A.; Shchukin, D.; Fedutik, Y.; Petrov, A. I.; Sukhorukov, G. B.; Möhwald, H. *Colloids Surf., A* **2003**, *224*, 175. (c) Yu, S.-H.; Cölfen, H.; Xu, A.-W.; Dong, W. *Cryst. Growth Des.* **2004**, *4*(1), 33.
- (10) (a) Volodkin, D. V.; Larionova, N. I.; Sukhorukov, G. B. *Biomacromolecules* **2004**, *5*, 1962.
- (11) Hamada, S.; Kudo, Y.; Okada, J.; Kano, H. *J. Colloid Interface Sci.* **1987**, *118* (2), 356.
- (12) Xia, Y.; Gates, B.; Yin, Y.; Lu, Y. *Adv. Mater.* **2000**, *12* (10), 693.

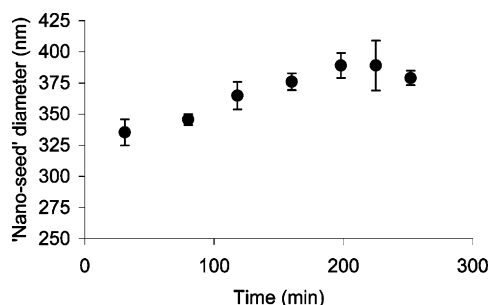


**Figure 1.** The relationship between nanoseed diameter and time.

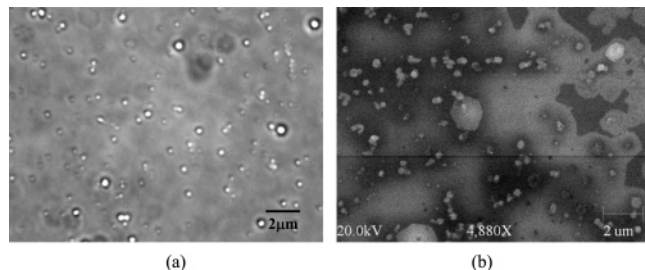


**Figure 2.** Images of nanoseeds for production of  $\text{MnCO}_3$  microparticles. (a) Bright-field optical microscopy and (b) SEM image.

### 3. Results and Discussion

Inorganic colloids are usually prepared via precipitation reactions, a process that often involves two sequential steps: nucleation and growth of the nuclei. To achieve monodispersity, these two stages must be strictly separated; specifically, nucleation should be avoided during the period of growth. According to this theory, the nanoseed solution was freshly prepared in our study as nuclei at low concentration to avoid crystal growth. The nuclei provided in the

subsequent reaction allow growth on tiny crystals, which again suppresses the undesirable nucleation procedure. As a result, monodisperse crystals form. By adjusting the number of nuclei per unit volume, different sizes of crystals may be obtained. The more nuclei used, the smaller the particles produced. For practical application, there is a limitation of the particle size range to obtain spherical and monodisperse particles. In  $\text{MnCO}_3$  particle production, particles with sizes less than  $1\ \mu\text{m}$  have broader size distribution, while particles bigger than  $10\ \mu\text{m}$  tend to be cubicle in shape.

**3.1. Characterization of Nanoseeds.** The size of nanoseeds prepared in our study could range from 200 to 700 nm as shown by particle sizing, and all can be used for the production of microscale  $\text{MnCO}_3$  particles. Particle size measurements prior to the fabrication of each batch of  $\text{MnCO}_3$  microparticles indicated a slight variation in nanoseed diameter over time as shown in Figure 1. The slight increase in nanoseed diameter could be the result of additional crystallization. Although the nanoseed solution was constantly stirred, aggregation was observed during the data acquisition at time 31, 80, 118, and 252 min, respectively, as indicated by the emergence of a bimodal distribution. However, aggregation was not observed during the remaining acquisition times by the appearance of a normal distribution, indicating that although aggregates were present, there was no correlation with time. The aggregate contribution to the overall measured intensity was approximately  $12.9 \pm 8.5\%$ , an indication that severe aggregation was not observed. It was found that the size of  $\text{MnCO}_3$  microparticles could be well controlled by adding different volumes of the nanoseed solution into  $\text{MnSO}_4$  solution before mixing with  $\text{NH}_4\text{HCO}_3$ .

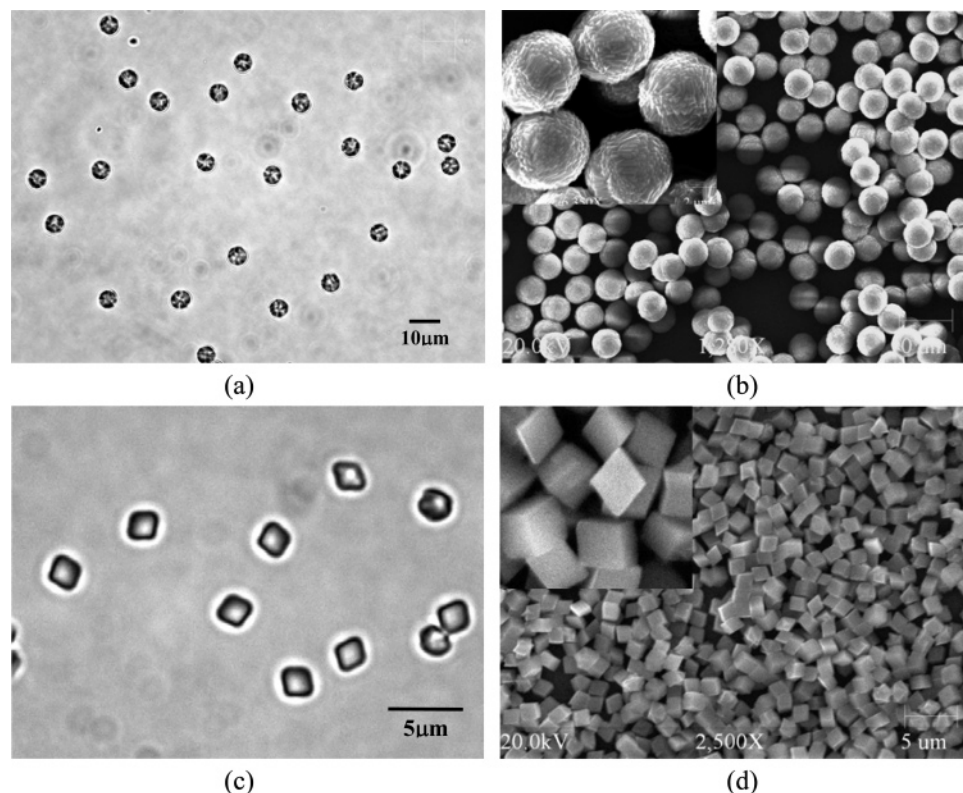


**Figure 3.** Images of  $\text{MnCO}_3$  microparticles. (a) Bright-field optical microscopy image of spherical  $\text{MnCO}_3$  particles, (b) SEM image of spherical  $\text{MnCO}_3$  particles, (c) bright-field optical microscopy image of cubicle  $\text{MnCO}_3$  particles, and (d) SEM image of cubicle  $\text{MnCO}_3$  particles.



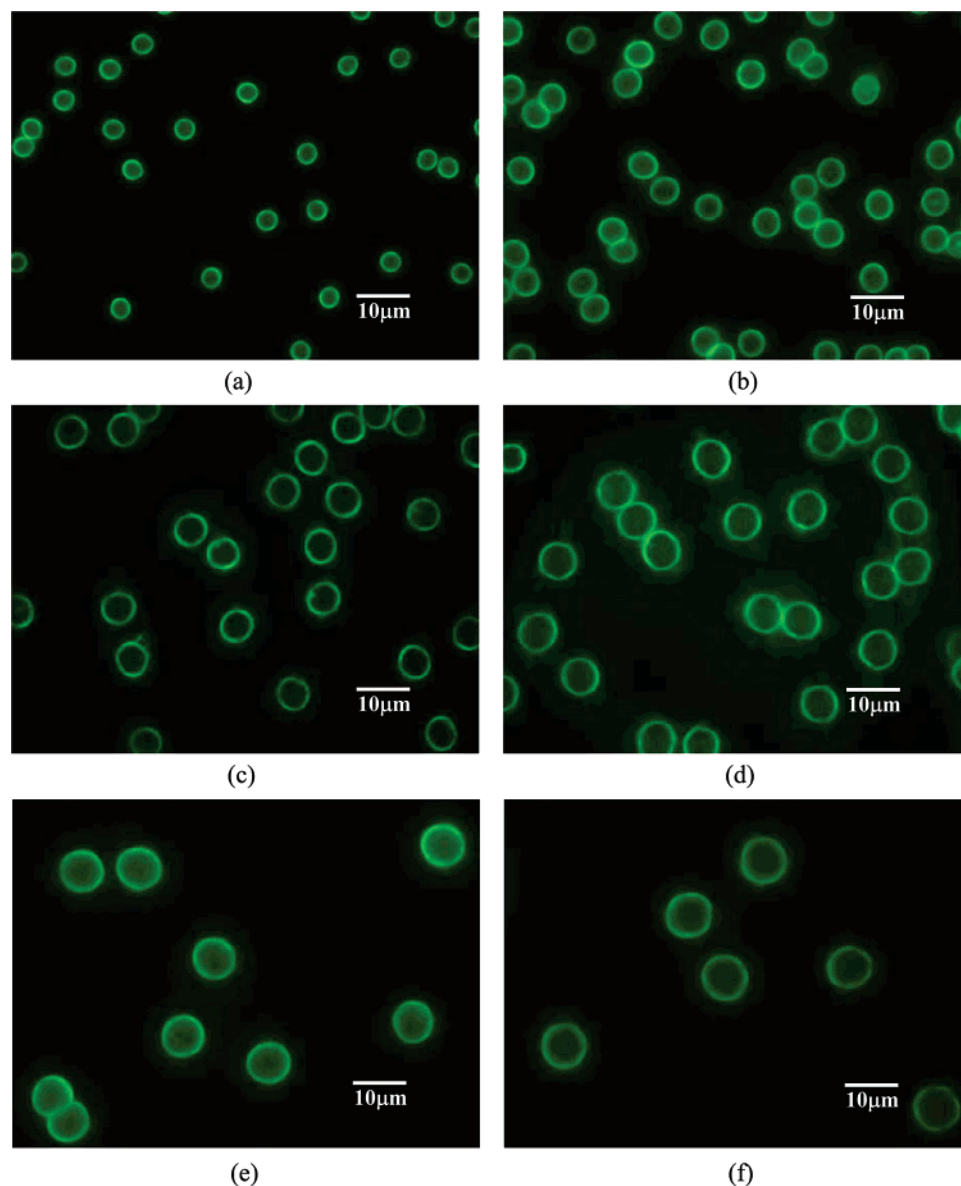


**Figure 4.**  $\text{MnCO}_3$  particles with different diameters, imaged with fluorescence microscopy (average diameter: (a)  $3.8\ \mu\text{m}$ , (b)  $5.3\ \mu\text{m}$ , (c)  $6.0\ \mu\text{m}$ , (d)  $6.9\ \mu\text{m}$ , (e)  $7.9\ \mu\text{m}$ , and (f)  $8.7\ \mu\text{m}$ ).

Without the nanoseed solution, the size of the  $\text{MnCO}_3$  microparticles is uncontrollable and a broad size distribution results, although the particle shape is still spherical when high-speed stirring is employed. Bright-field optical microscopy and SEM were used to image the nanoseeds, as shown in Figure 2a and 2b. The nanocrystals in Figure 2 are spherical in shape and range from 200 to 400 nm, which agrees with the particle sizing results. The nanoseeds are unstable and aggregate when dried, as observed in SEM images.

**3.2. Size Distribution of  $\text{MnCO}_3$  Microparticles.** The microparticles were observed under bright-field illumination with an oil immersion objective lens (Figure 3a). It can be seen that the crystals have spherical shape with rather uniform size distribution. It is believed that the homogeneous isotropic crystal growth on tiny crystal nuclei yields spherical shape and uniform distribution of the  $\text{MnCO}_3$  particles under strong stirring. SEM was used to further analyze the surface morphology and size distribution of  $\text{MnCO}_3$  particles (Figure 3b), with findings consistent with optical microscopy ob-

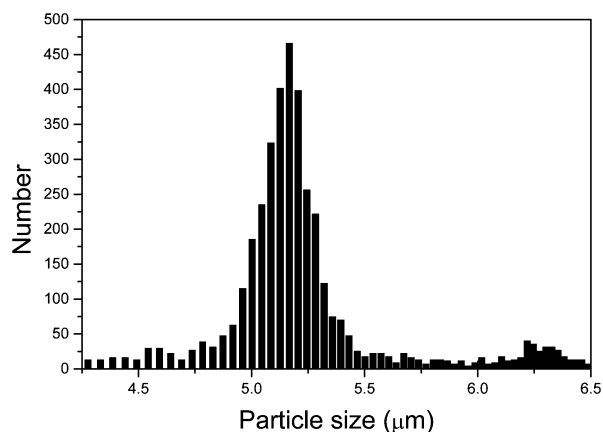


**Figure 5.** Coulter counting of  $\text{MnCO}_3$  microparticles.

servations (Figure 3a). In contrast, cubical crystals were obtained with slow or no stirring under otherwise identical reaction conditions (Figure 3c and 3d). Under higher magnification (inset in Figure 3b), it could be seen that the spherical particles were composed of tiny crystals, resulting

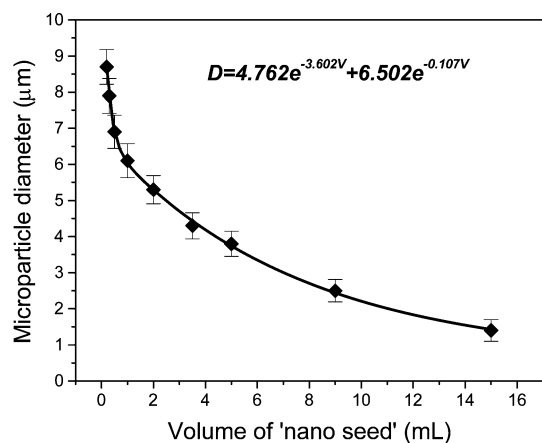


**Figure 6.** The relationship between particle diameter ( $D$ ) and volume of nanoseed solution ( $V$ ) used when synthesizing  $\text{MnCO}_3$  particles (error bars are one standard deviation,  $N > 3000$ ).

in somewhat rough surfaces. In contrast, the cubicle particles have very smooth surfaces.

Following production of  $\text{MnCO}_3$  particles, the common polyelectrolyte pair PSS/PAH was used to deposit multilayers on the inorganic template. The particles were coated with four bilayers of {PSS/FITC-PAH} to allow observation with fluorescence microscopy. Figure 4 contains a subset of fluorescence images of collected  $\text{MnCO}_3$  particles with polyelectrolyte coatings, showing average sizes from 3.8 to 8.7  $\mu\text{m}$ , which were achieved by varying the nanoseed volume. According to these experimental results, it is apparent that the size of  $\text{MnCO}_3$  microparticles can be well

controlled from 1 to 10  $\mu\text{m}$  by adding different volumes (0.1–20 mL) of the prepared nanoseed solution while maintaining a uniform size distribution. As expected, the particle size decreases when increasing the volume of nanoseed solution added.

A Coulter counter was used to further characterize the particle size distribution. A typical counter result shows that the mean particle size is  $5.29 \pm 0.41 \mu\text{m}$  (Figure 5), with 2 mL of nanoseeds used for particle production. The sample of particles is from the same batch used to generate Figure 4b. Additional experiments showed that  $\text{MnCO}_3$  particles were consistently monodisperse, with standard deviation of  $<0.5 \mu\text{m}$  ( $N > 3000$ ) (Figure 6). The empirical relationship between  $\text{MnCO}_3$  microparticle diameter ( $D$ ) and volume of nanoseed solution ( $V$ ) could fit a biexponential decay:  $D = 4.762 \cdot e^{-3.602V} + 6.502 \cdot e^{-0.107V}$  ( $R^2 = 0.9987$ ). Theoretically, the volume-dependent final size can be estimated using a cubic equation if some simple assumptions can be made. Assuming a constant nanoseed initial size  $r_0$  and constant nanoseed particle concentration  $C$ , the change in particle size can then be related to the total volume change in the spheres because of the crystallized  $\text{MnCO}_3$  if the total  $\text{MnCO}_3$  is also assumed to be constant. However, the practical nanoseeds are not very stable in size and tend to grow slowly over time. Because of the limitation that all the samples cannot be produced at the same time, the empirical relationship shows to fit biexponential decay better than cubic equation. According to our experimental results,  $V$  should

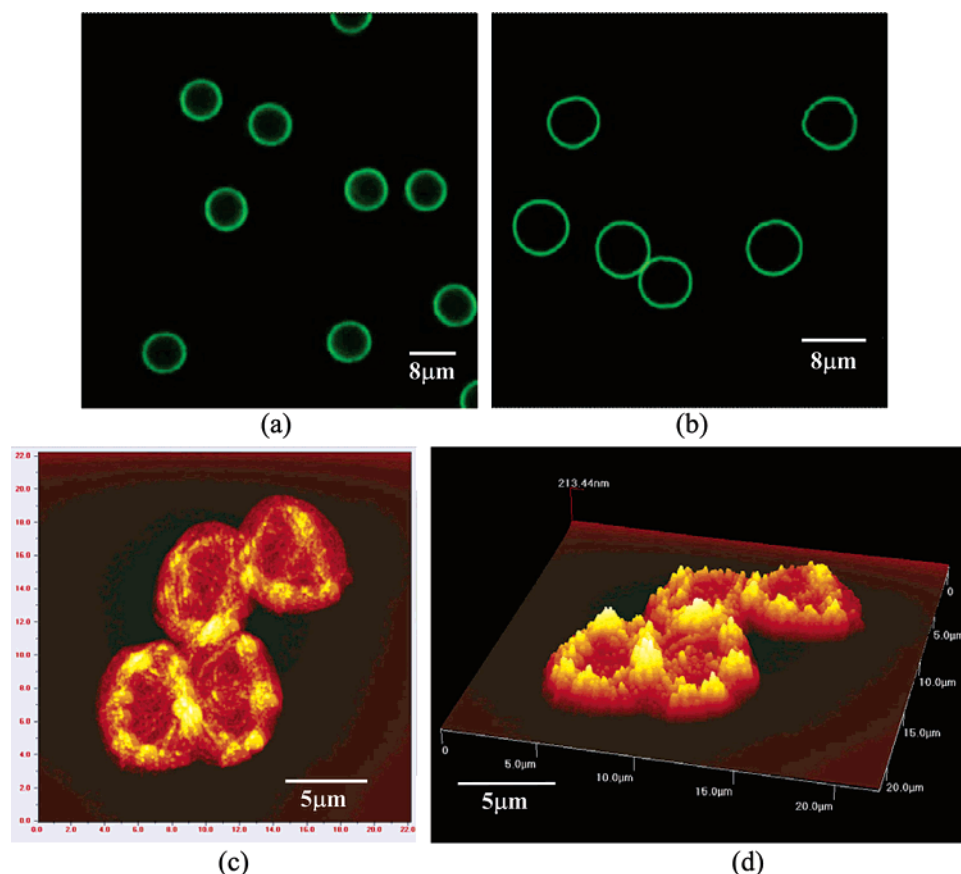


**Figure 7.**  $\text{MnCO}_3$  microparticles and capsules with four bilayers of {PSS/FITC-PAH}. (a) Confocal images of  $\text{MnCO}_3$  microparticles with multilayer coatings, (b) confocal images of capsules after dissolution of  $\text{MnCO}_3$  core, (c) AFM topography image of dried capsules, and (d) AFM 3-D image of dried capsules.

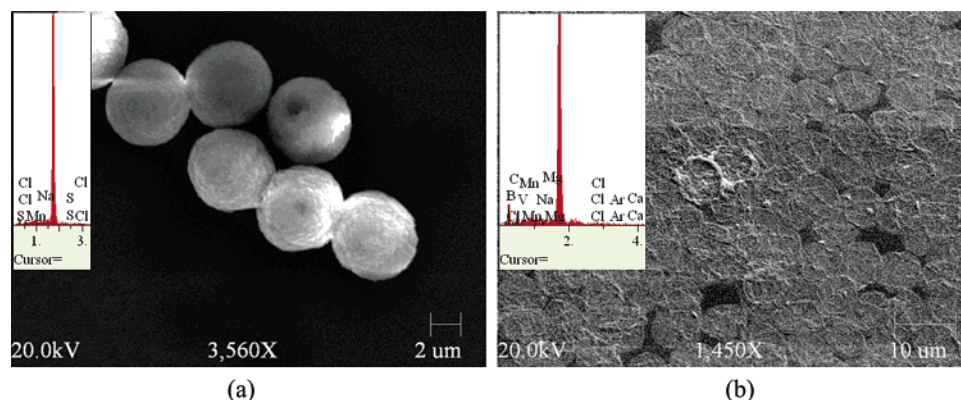


**Figure 8.** SEM-EDX analysis of (a)  $\text{MnCO}_3$  microparticles with four bilayers {PSS/PAH} and (b) microcapsules with cores dissolved by HCl and treated with EDTA solution.

be less than 20 mL, and  $D$  is in the range from 1 to 10  $\mu\text{m}$ , where monodisperse particles with spherical shape could be obtained. The particles with sizes less than 1  $\mu\text{m}$  have broader size distribution, while particles bigger than 10  $\mu\text{m}$  tend to be cubicle or irregular in shape.

**3.3. Fabrication of Polyelectrolyte Multilayers on  $\text{MnCO}_3$  Microparticles.** To investigate the potential of these  $\text{MnCO}_3$  crystals to serve as templates for size-controlled hollow capsule formation, the layer-by-layer (LbL) assembly of polyelectrolyte layers was monitored by electrophoretic mobility measurements. Four bilayers of {PSS/PAH} were deposited on  $\text{MnCO}_3$  cores, and the surface potential of the microspheres was observed to change regularly from 50 mV for  $\text{MnCO}_3$  cores and 40 mV for PAH to  $-35$  mV for PSS (data not shown here), indicating the formation of {PSS/PAH} $_4$  wall architecture.

The  $\text{MnCO}_3$  cores with multilayer coating comprising {PSS/PAH} $_4$  were then dissolved by exposure to HCl and EDTA solution, followed by rinsing with DI water. The coated  $\text{MnCO}_3$  particles and the capsules following the core dissolution were imaged with confocal microscopy (Figure 7a and 7b). The results again show narrow size distribution, efficiency of capsule formation, and integrity of microcapsules with nanoscale walls. Tapping mode atomic force microscopy was used to further confirm capsule formation by core removal. Capsules imaged with AFM (in the dry state) are presented in Figure 7c and 7d. The average height of the collapsed microcapsules was calculated to be  $\sim 40$  nm. Thus, each bilayer of the microcapsules is calculated to be 5 nm, which agrees with previous reports.<sup>1b,13</sup>

SEM-EDX was used to detect the presence of manganese before (Figure 8a) and after (Figure 8b) the dissolution of the cores. The particles with polyelectrolyte coating did not show a difference to uncoated  $\text{MnCO}_3$  microparticles in Figure 3b. After HCl/EDTA treatment, the  $\text{MnCO}_3$  cores

were dissolved. The left hollow polyelectrolyte multilayer microcapsules were collapsed to thin films when dried. The EDX result showed 12.76 wt % of manganese in  $\text{MnCO}_3$  microparticles with {PSS/PAH} $_4$  coating, while 0 wt % manganese (nondetectable) after the cores were dissolved by HCl and treated with EDTA solution.

Size-controlled monodisperse  $\text{MnCO}_3$  microparticles were therefore synthesized by using nanoseeds as nuclei for crystal growth, which shows high potential for commercial batch production. The microcapsules obtained after polyelectrolyte multilayer deposition on  $\text{MnCO}_3$  cores and HCl/EDTA treatment were spherical, uniformly distributed, and free of metal ions. These clean microcapsules are especially useful for encapsulating bioactive molecules, for example, enzymes, as biosensors, where uniform capsules provide homogeneous properties during encapsulation. In addition, availability of such particles can be quite useful for many more applications, such as their conversion into manganese oxide as solid electrode and catalyst,<sup>11</sup> rather than used as templates for polyelectrolyte multilayer capsule formation.

## Conclusion

Monodisperse manganese carbonate microparticles were synthesized, with tunable size ranging from 1 to 10  $\mu\text{m}$ , using a process that requires no separation procedure. It was found that the particle size can be easily adjusted by adding different volumes of nanoseed solution, prepared by mixing diluted  $\text{NH}_4\text{HCO}_3$  with  $\text{MnSO}_4$  solution. It was further verified that the manganese carbonate microparticles can be used as templates for efficient formation of uniform, smooth multilayer polyelectrolyte microcapsules. The microparticles prepared in this efficient manner should prove to be promising candidates to fabricate polyelectrolyte multilayer capsules for biomedical and other applications.

**Acknowledgment.** This work was supported by the National Institutes of Health (Grant #R01 EB00739-01).

CM048229R

(13) Estrela-Lopis, I.; Leporatti, S.; Moya, S.; Brandt, A.; Donath, E.; Möhwald, H. *Langmuir* **2002**, *18*, 7861.